Investigation of Shear Strength of Subbase-Subgrade Interface with Geosynthetics Reinforcement Utilizing A Large-Scale Direct Shear Test

Qais S. Banyhussan[1,a], Hanan A. hassan[1,b] and Badr A. Hamad [1,c*]

[1]Highway and Transportation Department, Mustansiriyah University, Baghdad, Iraq

[a] qaisalmusawi@uomustansiriyah.edu.iq, [b] ghassan_hanan@uomustansiriyah.edu.iq, and [c]edma017@uomustansiriyah.edu.iq,

*Corresponding author

Abstract. Geosynthetics are being used to strengthen road pavement. Geosynthetic inclusions improve pavement carrying capacity, maintenance costs, highway service life, reflective cracks, and undesirable large lateral and vertical deformations. The primary purpose of this research is to determine the effectiveness of geosynthetics (geogrids and geotextiles) in stabilizing the subgrade and reinforcing the base course layers in unpaved test sections. Determine the mechanical interaction of subgrade soils (clay and sand) and aggregate road base layers (subbase) with and without reinforcement. Compute the shear strength parameters (cohesion, friction angle, and interface coefficient factor). Therefore, Large-scale direct shear experiments in the laboratory were performed on subbase-subgrade materials with and without geosynthetics, under the applying normal of stresses (25, 50, 75, and 100) kPa, indicating the quantity overburden the pressure in paving. The present research uses a large-scale direct shear apparatus with an up square box (200 mm×200 mm×100 mm) and a bottom rectangular box (200 mm×250 mm×100 mm). A direct shear test was implemented by manufacturing this equipment. The results obtained from experiments showed that biaxial geogrid G1 has the best behavior for both (subbase-clay) and (subbase-sand) and has an interface shear coefficient factor more significant than unity and equal to 1.05 and 1.02, respectively.

Keywords: Geogrid; geotextile; LSD; shear test; shear strength; LVDT.

1. INTRODUCTION

The application of geotechnical engineering, especially in the design and stability assessment of geosynthetic-reinforced soil structures, is of the utmost importance for the interaction involving soils and geosynthetics. In addition, rapid urbanization will inevitably lead to an increase in the need for soil stabilizing techniques so that transportation infrastructure can be built atop subgrade deposits with lower shear strength as well as high compressibility. Geogrids offer strength by laterally restricting the foundation or sub-base and enhancing the system bearing capacity, reducing shear strains on the weak subgrade. Moreover, geogrid confinement enhances vertical stress distribution over the subgrade, reducing vertical subgrade deformation. More than 70 direct shear tests were performed to assess a liner system's interface shear strength properties using project-specific materials under site conditions [1]. Abu-Farsakh [2] examined the impact of dry density and moisture content on the cohesiveness of soil-geosynthetic interactions at thorough testing for direct shear. During direct shear testing, Liu [3] assessed the role of transverse ribs in the interaction between geogrid and the soil. For their soil-geogrid interfaces in direct shaer at large-scale device experiments, Liu [4] compared various setups of the shear box dimensions and concluded that a lower box of the same size as the upper box was the most appropriate. The primary benefits and drawbacks of each method were highlighted in [5]. Comprehensive investigations on theoretical, experimental, and computational methods for analyzing the interaction between geosynthetics and soils are presented and discussed. Basudhar [6] conducted an experimental investigation on the relationship between woven geotextiles and soils utilizing the direct shear test and two geotextiles with various weave textures and proposed non-linear structure modeling to forecast the interfaces' behavior before and after the peak.

To use a modified large-scale direct shear LSD apparatus, the interface shear strength characteristics of the aggregate of interfaces in geogrid-reinforced building and demolition were studied [7]. Various types of materials testing and other recent direct or interface shear test research studies can be found in the literature [8-11]. Based on the abovementioned gaps, additional research is needed on the interfacing parameters between road-base materials and geosynthetics for road-base reinforcement and subgrade stabilization. This research used single-stage testing to conduct a series of direct shear tests on road-based materials without and with the addition of geosynthetic reinforcement. Soil stabilization is the chemical and/or mechanical reduction of compression, contraction, swelling limits, and permeability to increase soil strength and durability [12-15].

2. MATERIAL USED

2.1 Subbase Material

The sub-base granular materials (SGM) Type B employed in this study were sourced from the AL-Nibaee area north of Baghdad. The physical and chemical properties of the subbase material are shown in Table 1.

© The Authors, published by EDP Sciences. This is an open access article distributed under the terms of the Creative Commons Attribution License 4.0 (https://creativecommons.org/licenses/by/4.0/).

Gradation and sieve analysis according to the permitted limits of the Iraqi specification of the subbase material (SCRB /R6, 2003) are exposed in Table 2 as well as in Figure 1.

Table 1: Physical and chemical properties of subbase materials.

Characteristics	Results	Limits of SCRB/R6,2003
Max. dry density (gm/cm^3)	2.198	Not limited
Organic matter, %	1.8	Max. 2
T.S.S, %	7	Max. 10
(SO_3) content, %	4.1	Max. 5
Gypsum content, %	8.815	Max. 10.75

Table 2: Gradations of the subbase material.

% Passing by the weight		
Size of the sieve (mm)	**Passing (%) used in the study**	**Limits of SCRB/R6, 2003**
75	100	-
50	100	100
25	90	75-95
9.5	63.4	40-75
4.75	40.46	30-60
2.36	34.43	21-47
0.3	20.76	14-28
0.075	5.96	5-15

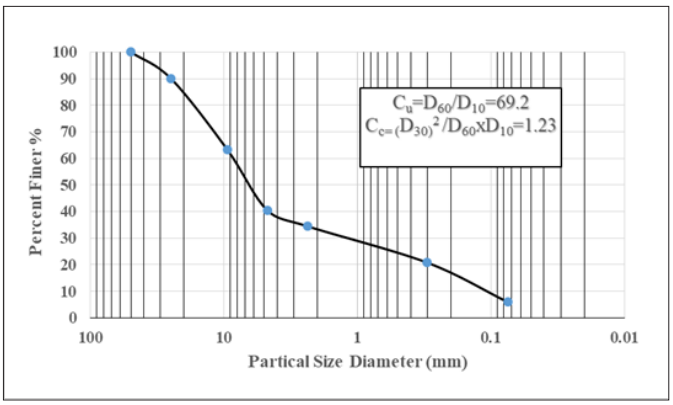

Figure 1: Grain size analysis of subbase.

2.2 Clay Soil

The clay soil was brought from the Tajiyat area north of Baghdad, Iraq. Physical tests were done on the soil, and it was assigned the soil classifications (CL) by the Unified of Soil Classification Systems USCS and according to ASTM (D2487-11) as well as (A-6) by AASHTO, ASTM (D3282-09). A grain size distribution and physical and chemical characteristics of the clay soil used in this study are illustrated in Figure 2 and Table 3.

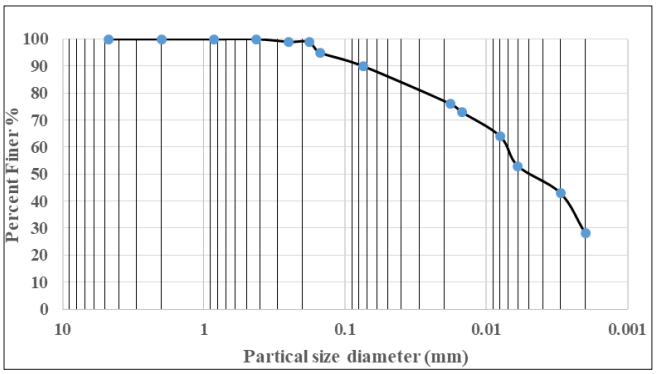

Figure 2: Grain size distribution for clay soil.

Table 3: Physical and chemical properties of clay soil

properties	Results	Specification requirement
Specific gravity	2.68	ASTM D 854 (2014)
Liquid limit (%)	40	ASTM D 4318 (2017)
Plastic limit (%)	14	ASTM D 4318 (2017)
Plasticity index (%)	26	ASTM D 4318 (2017)
Maximum dry density (g/cm^3)	1.72	ASTM D 1557-07
Optimum moisture content (%)	18.6	ASTM D 1557-07
CBR at 95% compaction	5	AASHTO T180 (4 min)
Organic matter (%)	1.89	(SCRB/R6,2003) (2 max)
T.S.S (%)	4.61	(SCRB/R6,2003) (10 max)
SO3 content (%)	1.64	(SCRB/R6,2003) (5 max)
Gypsum content (%)	3.52	(SCRB/R6,2003) (10.75 max)
Soil classification	A-6	AASHTO
Unified soil classification	CL	ASTM D-2487 (2017)

2.3 Sand Soil

Physical testing was performed on sandy soil transported from the Iraqi city of Karbala. Soil type is categorized as (SP) soil, according to AASHTO and the Unified of Soil Classification Systems (USCS) according to ASTM (D2487-11), as well as (A-3) soil ASTM (D3282-09). Used sand grain size distribution is displayed in Figure 3; its physical characteristics are exposed in Table 4.

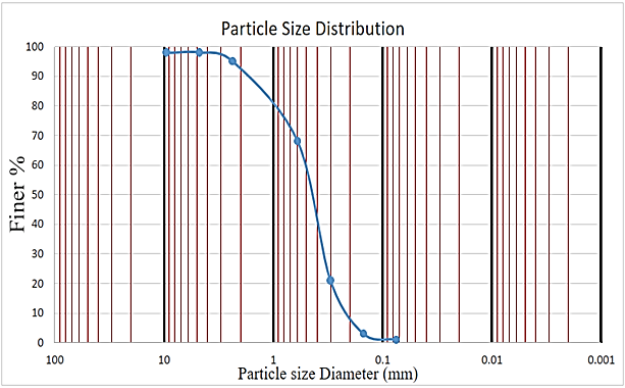

Figure 3: The sand particle size distribution.

Table 4: Properties of sandy soil.

Characteristics	Value	Specification	Characteristics	Value	Specification
Specific gravity	2.564	ASTM D854	Plasticity index (%)	N.P	ASTM D4318
Liquid limit (%)	-	ASTM D4318	Maximum dry density (g/cm^3)	1.831	ASTM D1557-07
Plastic limit (%)	N.P	ASTM D4318	-	-	-

2.4 Geosynthetic Reinforcement

The following four geosynthetic product categories, which are frequently utilized in pavement engineering for base reinforcement as well as subgrade stabilization, were chosen: Rectangular apertures geogrid (G1) and biaxial geogrid BX1100, Rectangular apertures geogrid (G2), SS2, PP welded (Square apertures geogrid G3), and HT380PPI (woven geotextile GT), as shown in Figure 4 and Tables 5 to 8 illustrated the characteristics of geosynthetics used in this research.

Table 5: Physical properties of the PP geogrid (Tensar International Co.).

The physical properties	Data	
Polymer	PP	
Color	White	
Polymer type	PP welded geogrid	
Rib shape	Rectangular	
Dimensional properties	**Unit**	**Dimensional properties**
Roll width	m	Roll width
Roll length	m	Roll length
Aperture size	mm	Aperture size
Minimum Average Tensile Strength Longitudinal Direction ≥ (kN/m)	40	
Minimum Average Tensile Strength Transverse Direction ≥ (kN/m)	40	

Table 6: Physical properties of the SS2 geogrid (Tensar Co.).

The physical properties	**Data**	
Polymer	PP	
color	Black	
Polymer type	SS2	
Rib shape	Rectangular	
Dimensional properties	**Unit**	**Data**
Aperture size	mm	28*40
WLR	mm	3
WTR	mm	3
tTR thickness of transverse ribs	mm	0.9
tLR thickness of longitudinal ribs	mm	1.2
Quality control Strength (longitudinal)		
Load at 2% strain (3)	kN/m	7.0
Load at 5% strain (3)	kN/m	14.0
Load at 2% strain (3)	kN/m	12.0
Load at 5% strain (3)	kN/m	23.0

Table 7: Physical and mechanical properties of Biaxial geogrid (Tensar International Co.).

The physical properties	**Data**		
Polymer	PP		
color	Black		
Polymer type	Biaxial geogrid		
Rib shape	Rectangular		
Index properties	**Units**	**MD Values**	**XMD Values**
Aperture Dimensions	mm	25	33
Rib Thickness	mm	0.76	0.76
Tensile Strength @ 2% Strain	Kn/m	4.1	6.6
Tensile Strength @ 5% Strain	Kn/m	8.5	13.4
Ultimate Tensile Strength	Kn/m	12.4	19.0

Table 8: Properties of the HT380PPI geotextile (Shandong Hassan Chinas Co.).

The physical properties	**Unit**	**specification**
Tensile strength MD	KN/m	70
Tensile Strength CD	KN/m	80
Elongation MD/CD	%	< 13%
Equivalent opening size (O_{90})	mm	0.48
Permeability (Q_{50})	$L/m^2/sec$	58
UV resistance	%	90

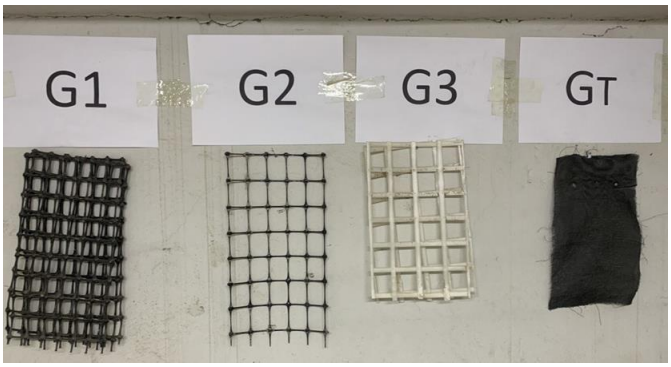

Figure 4: Geosynthetic reinforcement that was used in the study.

3. THE EQUIPMENT and SPECIMENS' PREPARATION

3.1 Testing of Equipment

The present study used a large-scale direct shear apparatus with variable normal stresses (25 kPa, 50 kPa, 75 kPa, and 100 kPa) manufactured by [16] with some modifications. It comprises an upper square steel

box measuring 200 * 200 * 100 mm and a lower rectangular steel box measuring 200 * 250 * 100 mm. The low box size was kept greater than the up box shown in Figure (5) to maintain a constant shear area during the testing. Two horizontal arms were fastened to the machine frame to stop the upper of a shear box from moving. Guide rails were positioned at the base plate, where the low shear box was mounted, to allow for frictionless movement. The lower box was pushed down, and the sample was sheared using a horizontal hydraulic jack. Before each test, the internal walls of the box were covered with a lubricating oil cover to lessen friction at the sidewalls.

Moreover, the device contains a floating upper box separating the higher from the lower shear box. A robust steel plate was utilized as the loading plate, coupled to a loading lever, and the usual load was applied through it. A dead weight served as a counterbalance. A motor, control panel, and gear system powered by a hydraulic jack system sheared the test specimen while maintaining a controlled, consistent shear displacement rate.

Figure 5: The large-scale direct shear device.

Two horizontal loadcells with a capacity of 50 kN and two linear varying differentiation transducers (LVDTs) with such a range of (50 mm) made up the measuring apparatus. The sample was sheared, and the vertical and lateral deformations were measured using LVDTs. A Data Acquisition System automated the measurements (DAQ). As shown in Figure 6, during interface testing, the reinforcement was positioned at the junction of the upper and bottom boxes and clamped firmly to the lower box.

Figure 6: Clamping system for geosynthetics.

3.2 Sample Preparation

The appropriate optimal moisture contents were added to the dry materials and carefully mixed to create the samples for the direct shear tests. By compacting the first soil preparation to the targeted unit of weight inside the shear box, the soil for the program's extensive direct shear testing is ready. Three layers are compressed for soil. The clay, as well as the subbase, are compacted with an electric vibrator and a conventional Proctor hammer, as well as the sandy soil is compacted by hand-striking steel of plate that was put on top of the soil until it reaches the desired unit weight as shown in Figure 7. The specimen was compressed in the shear box before being mounted in the apparatus to safeguard the sensitive electrical controllers.

The required mass of wet soil for each layer was determined, precisely measured, and then uniformly compacted to the required height for the required dry density. Before specimens were compacted in the shear box, the upper and lower boxes of the shear box were connected by keeping the two alignment pins in position to ensure that the top and bottom halves were correctly aligned.

The geosynthetic specimen is set atop the lower shear box and secured to its front edge by two bolts and a steel clamping block. Four boxes were used for this testing, as illustrated in Figure 8. Normal pressures of (25, 50, 75 kPa, and 100 kPa) were applied to the sample before it was sheared, and it was given 5 minutes to consolidate [17].

A B

Figure 7: Compaction of sample: (a) used steel plate for uniformity, (b) used steel plate and plastic hummer.

Once compression under each normal stress was complete, shearing was started under a constant rate equal to (1mm/min) until the shear of displacement reached 30 mm (10 % shear strain) [18], [3], [4], [19]. Shear load, vertical displacement, and shear displacement were measured and recorded as the shearing process occurred.

Figure 8: Set of boxes used in the present study.

4. TESTING PROGRAM

Direct shear measurement to simulate interface subgrade stabilization (40 tests). This series of tests was designed to assess the interface parameters for both road-base and sub-grade enhanced with geosynthetics, start comparing the performance of the four different kinds of geosynthetics implanted here between road-base and subgrade with the case of an unreinforced road-base subgrade, and assess the impact of various soil types in the lower half of the shear box on the interaction shear stress. According to [ASTM D3080], direct shear testing on geotechnical materials (soil-soil) was performed.

According to [ASTM D5321], modified direct shear testing on soil-geosynthetic samples was performed. In order to conform with the [ASTM D5321] interfaces test method, the box size must be at least five times larger than the reinforcement's aperture. This ratio was determined to be 6.1 for (G1) geogrid reinforcements, 5 for (G2) geogrid reinforcements, and 5 for (G3) geogrid reinforcements.

5. FAILURE OF CRITERION

1- ASTM D3080 (2011) states that the specimen must be sheared to a horizontal displacement of at least 10% of the box's dimension, or 20 mm for a 200 mm-wide shear box.

2- The test may be stopped early if the desired shear stresses have been attained, or it may continue until the displacement reaches 75 mm or some other value set by the user, both of which are in line with ASTM D5321M (2014).
3- The shear displacements were limited to 10% shear strain and 30 mm shear displacement to avoid too much top cap warping and possibly wrong results [20]. These criteria were used in this study.

6. RESULTS AND DISCUSSION

6.1 Peak Shear Strength Envelopes and Shear Stress-Horizontal Displacement Curves

Interface shear stress tests with the inclusion of the four kinds of geosynthetics were performed at the specified unit of weight as well as optimum moisture of contents on the subbase-subgrades soil (clay and sand). For the clay-subbase interface, Figure 9 shows the difference between not. The content of these forms is initially included in the calculations to increase the attached figures for (shear stress-horizontal displacement) curves. We are satisfied with presenting the shear stress-horizontal displacement curves for each test at the applied normal stress of 50 kPa. For the four instances being considered, the interfacial shear stress curves showed a similar pattern of behavior. The figures show that increasing normal strength increases shear stresses for all cases. Furthermore, Figure 10 illustrates the shear stress for the sand-subbase interface. Figures 11 and 12 show the Mohr–Coulomb shear strength envelopes at peak. The shear strength parameters for each case are summarized in Tables 9 and 10.

In subbase-subgrade samples without reinforcement, the interface shear stresses rise with the horizontal displacement until they reach a peak and then oscillate after that. When aggregate particles are sheared, they rearrange themselves, and their levels of interlocking vary, which causes oscillations. However, the junction shear stress-horizontal movement curves of the subbase-subgrade example with geosynthetics do not exhibit a distinct peak even at a comparatively low normal stress of 50 kPa. Figures 11 and 12 show straight lines fitted through Mohr-Coulomb shear strength regions generated by the highest shear stresses. Straight lines fitted through the highest shear stresses produced Mohr-Coulomb shear-strength envelopes. The maximum shear strength range of subbase-subgrade examples with geogrids G1 is greater than that of an unreinforced subbase-subgrade sample due to the effects of particle-grid interlocking. Because of the smooth surface of the geotextile, Subbase-Gt-Subgrade has the lowest interface shear strength under several applied normal stresses. The three distinct geogrid types (G1, G2, and G3) used to support the subgrade, and road base have surprisingly similar shear stress curves because the three geogrids' opening area ratios are similar.

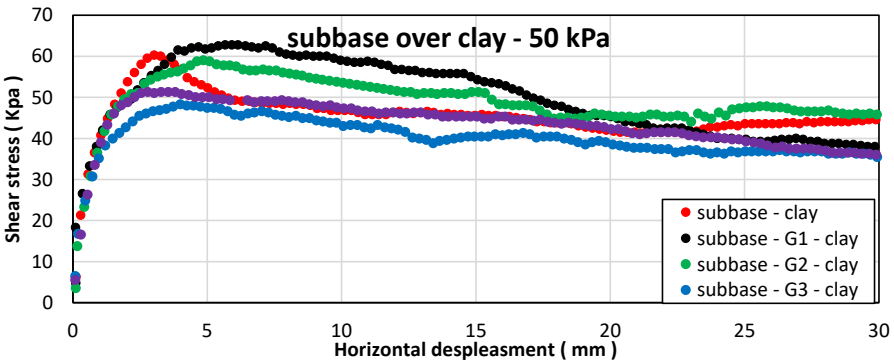

Figure 9: Modulation of shear stress of horizontal displacement for (sub-base over clay).

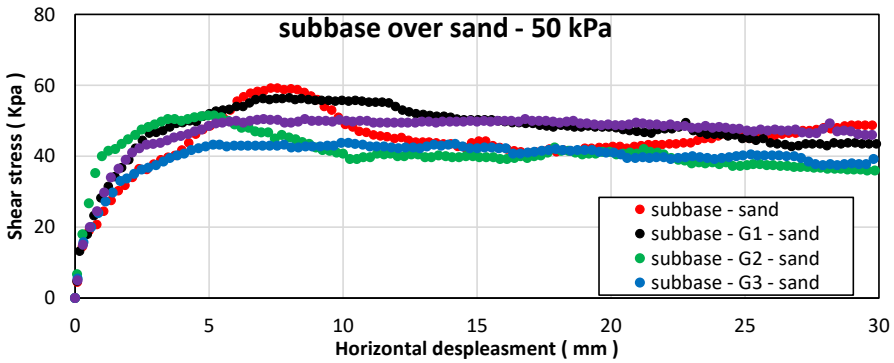

Figure 10: Modulation of shear stress of horizontal displacement for (sub-base over sand).

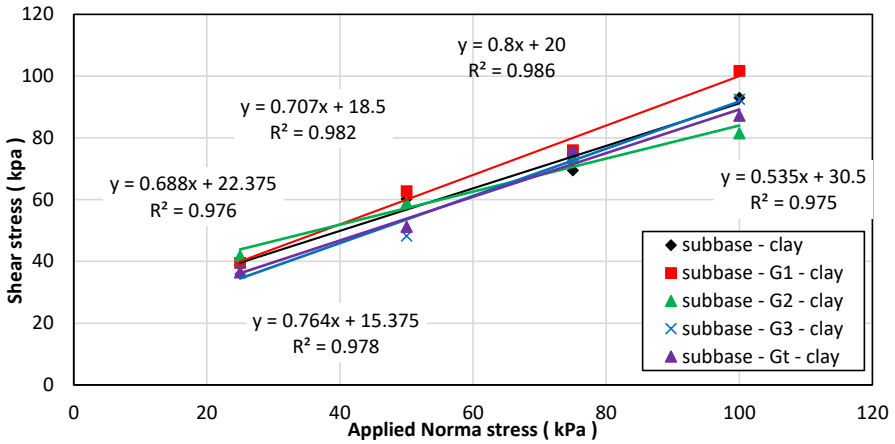

Figure 11: Envelopes of Mohr-Coulomb interface shear strength (subbase over clay).

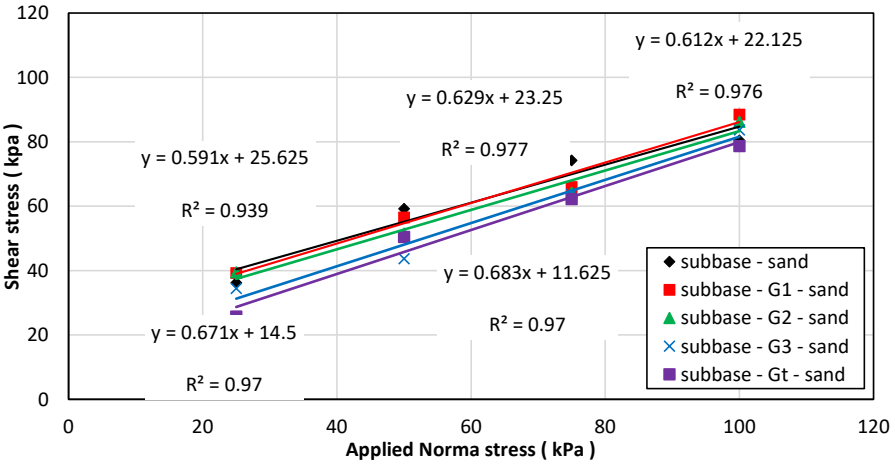

Figure 12: Envelopes of Mohr-Coulomb interface shear strength (subbase over sand).

Table 9: Shear strength characteristics of (sub-base over clay).

	Shear strength (peak) (kPa) $\tau = c + \sigma(tan\varphi)$				Cohesion c, (kPa)	Friction angle ϕ (degree)
Materials	**σ = 25**	**σ = 50**	**σ = 75**	**σ = 100**		
Subbase-Clay	40.46	58.54	76.63	94.71	22.38	35.88
Subbase-G1-Clay	40.75	61.50	82.25	103.00	20.00	39.69
Subbase-G2-Clay	43.75	57	70.25	83.50	30.50	27.92
Subbase-G3-Clay	33.71	52.04	70.38	88.71	15.38	36.25
Subbase-GT-Clay	35.42	52.33	69.25	86.17	18.50	34.08

Table 10: Shear strength properties of (subbase over sand).

Materials	Shear strength (peak) (kPa) $\tau = c + \sigma(tan\varphi)$				Cohesion c, (peak) (kPa)	Friction angle ϕ, (peak) (degree)
	σ = 25	**σ = 50**	**σ = 75**	**σ = 100**		
Subbase-Sand	40.38	55.13	69.88	84.63	25.63	30.54
Subbase-G1-Sand	39.67	65.08	72.50	88.92	23.25	33.29
Subbase-G2-Sand	37.71	53.29	68.88	84.46	22.13	31.94
Subbase-G3-Sand	30.92	47.33	63.75	80.17	14.50	33.29
Subbase-Gt-Sand	29.29	46.96	64.63	82.29	11.63	35.25

6.2 Interface Shear Strength Coefficient

The interface between the behavior of geosynthetics as well as the soil can be described by the coefficient of soil-reinforcement friction [4,21-23]. The following equation yields the interface's shear strength coefficient.

$$\eta = \tau_{reinforced} / \tau_{unreinforced} \quad (1)$$

Where η is the coefficient of interface shear strength, $\tau_{reinforced}$ as well as $\tau_{unreinforced}$ shear strength values are calculated from unreinforced and reinforced DST, respectively.

An interface shear stress coefficient higher than unity indicates geogrids' beneficial effects in reinforced soil-aggregate systems. On the other hand, inadequate aggregate particle size in proportion to geogrid aperture size, which leads to an interfacial shear strength coefficient below unity, is attributed to the lack of adequate aggregate particle-geogrid interlocking [24]. Table 11 summarizes the average coefficients of interface shear strength and the observed peak coefficients of interface shear strength for the normal stresses of 25, 50, 75, and 100 kPa. Geogrids frequently generate more interaction shear stress than geotextiles because of the link in geogrid apertures.

Table 11: Peak interface shear strength coefficients for normal stresses 25, 50, 75, and 100 kPa for roadbase-subgrade interface samples.

Materials	$\eta = \tau_{reinforced} / \tau_{unreinforced}$				
	σ = 25	σ = 50	σ = 75	σ = 100	Average η_{peak}
Subbase-G1-Clay	1.01	1.05	1.07	1.09	1.05
Subbase-G2-Clay	1.08	0.97	0.92	0.88	0.96
Subbase-G3-Clay	0.83	0.89	0.92	0.94	0.89
Subbase-GT-Clay	0.88	0.89	0.90	0.91	0.90
Subbase-G1-Sand	0.98	1.02	1.04	1.05	1.02
Subbase-G2-Sand	0.93	0.97	0.99	1.00	0.97
Subbase-G3-Sand	0.77	0.86	0.91	0.95	0.87
Subbase-Gt-Sand	0.73	0.85	0.92	0.97	0.87

The interaction coefficient for all geosynthetics used in this study increased when the normal strength increased at the (clay-subbase) and (sand-subbase) interface. However, the behavior of the interaction coefficient of (subbase-G2-clay) appears to have a different trend, where increasing normal stress leads to a decrease in the interaction. This may be related to inadequate interlock between large particles of sub-base in the opening area of geogrid. In general, the range of the interface the shear strength of coefficients for various soil/aggregate-geogrid interfaces described in the literature are 0.83-0.90 and 0.95-1.04 for gravel-geogrid and sand-geogrid interfaces, respectively [24]. (1.34–1.44) for the clay–sand–geogrid interface [25], (0.93–1.01) for the sand–geogrid interface [4], (1.00–1.14) for clay–sand–geogrid interface [26], (0.90–1.16) for ballast–geogrid interface [27], (0.66–1.60) for construction and demolition aggregate–geogrid interface [7] as well as (1.01–1.29) for sub-ballast (sand and gravel)–geogrid interface [28]. For the soil-aggregate-geogrid samples evaluated in this study, the measured interfacial shear strength coefficients are in good agreement with the range of values described in the literature. All tests have coefficients of interaction (η) greater than 0.7, showing good bonding between the geosynthetics and the soil under test [29].

7. CONCLUSIONS

Depending on thorough testing of the chosen subbase across several subgrade soil types, clay as well as sandy soil, and a series of large-scale direct with four types of geosynthetics G1, G2, G3, and GT, the following findings have been reached:

- It can be seen that the installation of geosynthetics reduces the apparent cohesion of the materials from 22.38 kPa for clay-subbase, where the interfaces friction angle and adhesive were found to be (35.88°) and (22.38 kPa), respectively (without reinforcement) to be 20 and 15.38 kPa for G1 and G3 respectively. At the same time, it increased with G2 from (22.38 to 30.50 kPa). However, it increases the friction angle slightly to 39.69° and 36.25° for G1 and G3 and decreases with G2 and GT to 27.92° and 29.83°.
- The friction and adhesion angle for the sand-subbase interface was 30.54° and 25.63 kPa without reinforcing. Using geosynthetics decreases the apparent cohesion to 23.25, 22.13, 14.50, and 11.63 kPa for G1, G2, G3, and GT. However, it increases the angle of friction to be 33.29°, 31.94°, 33.29° and 35.25° for G1, G2, G3, and GT, respectively.
- The interaction coefficient for all geosynthetics used in this study increased when the normal applied stress increased at the (clay-subbase) and (sand-subbase) interface, as illustrated in Table 11. However, the behavior of the interaction coefficient of (subbase-G2-clay) appears to have a different trend, where increasing normal stress leads to a decrease in the interaction.
- The results obtained from experiments showed that biaxial geogrid G1 has the best behavior for both (subbase-clay) and (subbase-sand) and has an interface shear coefficient factor greater than unity and equal to 1.05 and 1.02, respectively.

- Subbase-Gt-Subgrade has the lowest interface shear strength under several applied normal stresses. In all cases, the value of (η) is less than unity. The values obtained are (0.90) for (subbase-clay) and (0.87) for (subbase-sand).
- 6-When the effects of the four different types of geosynthetics assessed on contact shear strength are compared, geogrids frequently generate the most interaction with the shear stress than geotextiles. The soil-geotextile interaction is smaller than that of the soil-soil interface due to the smooth surface of the geotextiles, which greatly reduces interface shear stress. Therefore, extra consideration should be given to the geotextile-reinforced soils when sliding along contact is more likely to occur.
- The three types of geogrids (G1, G2, and G3) used to support the subgrade and road base have similar behavior in the shear stress-horizontal displacement curves, and the reason for this is attributed to the convergence of these three types in the size of the openings as mentioned in the characteristics of these geogrids in Table 5 to Table 8.

REFERENCES

[1] BERGADO, D. T., et al. Evaluation of interface shear strength of composite liner system and stability analysis for a landfill lining system in Thailand. Geotextiles and Geomembranes. 2006; 24(6): 371-393.
[2] Abu-Farsakh M, Coronel J, Tao M. Effect of soil moisture content and dry density on cohesive soil–geosynthetic interactions using large direct shear tests. J Mater Civ Eng. 2007;19(7):540–9.
[3] Liu CN, Zornberg JG, Chen TC, Ho YH, Lin BH. Behavior of geogrid-sand interface in direct shear mode. J Geotech geoenvironmental Eng. 2009;135(12):1863–71.
[4] Liu CN, Ho YH, Huang JW. Large scale direct shear tests of soil/PET-yarn geogrid interfaces. Geotext Geomembranes. 2009;27(1):19–30.
[5] Palmeira EM. Soil–geosynthetic interaction: Modelling and analysis. Geotext geomembranes. 2009;27(5):368–90.
[6] Basudhar PK. Modeling of soil–woven geotextile interface behavior from direct shear test results. Geotext Geomembranes. 2010;28(4):403–8.
[7] Arulrajah A, Rahman MA, Piratheepan J, Bo MW, Imteaz MA. Evaluation of interface shear strength properties of geogrid-reinforced construction and demolition materials using a modified large-scale direct shear testing apparatus. J Mater Civ Eng. 2014;26(5):974–82.
[8] Piratheepan J, Arulrajah A, Disfani MM. Large-scale direct shear testing of recycled construction and demolition materials. Adv Civ Eng Mater. 2013;2(1):25–36.
[9] Chen X, Zhang J, Xiao Y, Li J. Effect of roughness on shear behavior of red clay–concrete interface in large-scale direct shear tests. Can Geotech J. 2015;52(8):1122–35.
[10] Arulrajah A, Horpibulsuk S, Maghoolpilehrood F, Samingthong W, Du YJ, Shen SL. Evaluation of interface shear strength properties of geogrid reinforced foamed recycled glass using a large-scale direct shear testing apparatus. Adv Mater Sci Eng. 2015.
[11] Ferreira FB, Vieira CS, Lopes MDL. Direct shear behaviour of residual soil–geosynthetic interfaces–influence of soil moisture content, soil density and geosynthetic type. Geosynth Int. 2015;22(3):257–72.
[12] Al-Murshedi AD, Karkush MO, Karim HH. Collapsibility and shear strength of gypseous soil improved by nano silica fume (NSF). In: Key Engineering Materials. Trans Tech Publ. 2020.
[13] Karkush MO, Al-Murshedi AD, Karim HH. Investigation of the impacts of nano-clay on the collapse potential and geotechnical properties of gypseous soils. Jordan J Civ Eng. 2020;14(4).
[14] AL-Shamaa MFK, Sheikha AA, Karkush MO, Jabbar MS, Al-Rumaithi AA. Numerical modeling of honeycombed geocell reinforced soil. In: Modern Applications of Geotechnical Engineering and Construction: Geotechnical Engineering and Construction. Springer. 2021.
[15] Karkush MO, Almurshedi AD, Karim HH. Investigation of the Impacts of Nanomaterials on the Micromechanical Properties of Gypseous Soils. Arab J Sci Eng. 2023;48(1):665–75.
[16] Sahib Banyhussan Q, Mancy Mosa A, Nasser Hussein A, Jasim Sigar E. Evaluating the Shear Strength of Subbase-subgrade Interface Using Large Scale Direct Shear Test. Int J Innov Eng [Internet]. 2023 Mar 13;3(1 SE-Original Research):35–47. Available from: https://ijie.ir/index.php/ijie/article/view/96
[17] Umashankar B, Hariprasad C, Mouli SS. Interface properties of metal-grid and geogrid reinforcements with sand. In: IFCEE. 2015.
[18] Alfaro MC, Miura N, Bergado DT. Soil-geogrid reinforcement interaction by pullout and direct shear tests. Geotech Test J. 1995;18(2):157–67.
[19] Vieira CS, Pereira PM. Interface shear properties of geosynthetics and construction and demolition waste from large-scale direct shear tests. Geosynth Int. 2016;23(1):62–70.
[20] Xu Y, Williams DJ, Serati M. Investigation of shear strength of interface between road-base and geosynthetics using large-scale single-stage and multi-stage direct shear test. Road Mater Pavement Des. 2020;21(6):1588–611.
[21] Bergado DT, Chai JC, Abiera HO, Alfaro MC, Balasubramaniam AS. Interaction between cohesive-frictional soil and various grid reinforcements. Geotext Geomembranes. 1993;12(4):327–49.
[22] Tatlisoz N, Edil TB, Benson CH. Interaction between reinforcing geosynthetics and soil-tire chip mixtures. J Geotech Geoenvironmental Eng. 1998;124(11):1109–19.
[23] Lee KM, Manjunath VR. Soil-geotextile interface friction by direct shear tests. Can Geotech J.

2000;37(1):238–52.
[24] Sakleshpur VA, Prezzi M, Salgado R, Siddiki NZ, Choi YS. Large-scale direct shear testing of geogrid-reinforced aggregate base over weak subgrade. Int J Pavement Eng. 2019;20(6):649–58.
[25] Cazzuffi D, Picarelli L, Ricciuti A, Rimoldi P. Laboratory investigations on the shear strength of geogrid reinforced soils. In: GEOSYNTHETIC SOIL REINFORCEMENT TESTING PROCEDURES PAPERS PRESENTED AT A SYMPOSIUM HELD ON 19 JANUARY 1993 IN SAN ANTONIO, TEXAS, EDITED BY SCJ CHENG(SPECIAL TECHNICAL PUBLICATION (STP) 1190). 1993.
[26] Kamalzare M, Ziaie-Moayed R. Influence of geosynthetic reinforcement on the shear strength characteristics of two-layer sub-grade. Acta Geotech Slov. 2011;8(1):39–49.
[27] Indraratna B, Hussaini SKK, Vinod JS. On the shear behavior of ballast-geosynthetic interfaces. Geotech Test J. 2012;35(2).
[28] Biabani MM, Indraratna B. An evaluation of the interface behaviour of rail subballast stabilised with geogrids and geomembranes. Geotext Geomembranes. 2015;43(3):240–9.
[29] Coronel JJ. Frictional interaction properties between geomaterials and geosynthetics. Louisiana State University and Agricultural and Mechanical College. 2006.